J. Fluid Mech. (1984), *vol.* 140, *pp.* 355–372
Printed in Great Britain

A conditional-sampling study of the interaction of two turbulent wakes

By G. FABRIS†
Illinois Institute of Technology, Chicago, Illinois

(Received 3 September 1982 and in revised form 21 October 1983)

Measurements were taken of a developing complex turbulent flow formed by the merging of two far turbulent wakes of equal cylinders. The lower wake only was slightly heated, permitting the use of the conditional-sampling technique to study the interaction of the two wakes in detail. A special four-wire probe (Fabris 1978) enabled simultaneous uncontaminated measurement of all three instantaneous velocity components and temperature. The single-wake data of Fabris (1979) served as a reference. The interaction of the two single turbulent wakes resulted in a striking enhancement of the lateral transfer of heat. Undulations of the thermal interface are significantly wider laterally, but shorter streamwise than in the basic single wake. Lateral velocities of the heated and the unheated intermittent lumps are amplified two- to threefold by the interaction process. Levels of all three components of the kinetic energy of turbulence reach their highest relative maxima in the heated zones as they cross the upper cold wake. These maxima are higher than appropriate conventional or conditional maxima in the single wake. In addition to physical insights into the phenomena of turbulent flow, the data should be useful in refining and validating predictive methods, possibly spurring their further development.

1. Introduction

The term complex turbulent flow is defined by Bradshaw (1976) as flow with externally applied rates of strain or interaction of two or more basic turbulent flows. Except in the last few years, almost no detailed experimental investigation of such flows has been reported, because not even in the case of simple flows are the parameters sufficiently well known. However, most flows of engineering interest are complex, so that interest in documenting and predicting them is rapidly growing. Scientific investigations of such flows should shed more light on the mechanisms of the interaction in terms of the structure of the simpler component flows.

Some experimental investigations of such flows have been reported. Hanjalic & Launder (1972) studied, rather conventionally, the fully developed flow in a two-dimensional channel with walls of drastically different roughness which created an intriguing asymmetric flow. Palmer & Keffer (1972) investigated the development of an asymmetric wake. Fabris & Fejer (1974) studied confined mixing of 31 hexagonally arranged parallel jets. Also of interest is the work of Chevray & Kovasznay (1969) on the near and intermediate wake of a long thin plate where two opposing turbulent boundary layers relax asymptotically to the limiting case of a two-dimensional wake.

Through the pioneering efforts of Bradshaw's group at Imperial College, some

† Present address: Transamerica Delaval Inc., Biphase Energy Systems, Santa Monica, California; also University of California, Los Angeles.

detailed conditional sampling studies of complex turbulent flows are being conducted. Recently reported results are those by Dean & Bradshaw (1976), Andreopoulos & Bradshaw (1980) and Weir, Wood & Bradshaw (1981) on the interaction of two shear layers forming a duct flow, plane wake and jet. These three flows are actually basic flows, and their formation has been studied in the references mentioned above.

In the present study a 'new' complex flow was formed by the merging of two basic far plane turbulent wakes. Very slight heating of one of the wake-forming cylinders provided the tracer discrimination for the application of conditional sampling. A detailed study reported by Fabris (1979) of the basic single warm wake provided the basis against which to compare the merging process.

Flow-visualization studies can provide initial insight, incentive and direction for further quantitative studies of complex turbulent flows. Domptail, Bonmarin & Dumas (1978) have, for example, provided beautiful multicolour photographs depicting the interaction of vortices shed from two very closely spaced cylinders and the formation of an asymmetric near wake. Quantitative studies are needed also to explain further the intrinsic physics involved and to provide data for the development of better engineering prediction methods. In recent years Libby (1976) and Pope (1983) were among the few to conceive and offer new prediction methods based on conditional-sampling distinction between interacting potential and turbulent flow. It would be most interesting and beneficial to try to extend one of these novel methods to interactions of two turbulent flows. Data presented in this study should provide valuable guidance in such a venture.

Conditionally sampled data were taken at $x/D = 200$ and 400. For brevity, only the second location will be analysed in detail in this paper. The normalizing factors for the figures are $U_R = 6.46$ m/s, $\Theta_R = 0.4227$ °C and $D = 6.2484$ mm.

2. Experimental arrangement and technique

The experimental arrangement, technique, and supporting diagnostic experiments were described by Fabris (1979). Details of the test section are given in figure 1. The wake-generating cylinders are of diameter $D = 6.2484$ mm. The lower cylinder was heated slightly; this resulted in a maximum wake overheat at $x/D = 400$ of only 0.34 °C. Extensive and careful diagnostic experiments revealed no buoyancy. The lateral spacing of the axes of the two cylinders was selected equal to $8D$. In this way the individual initial wakes were independently formed and undistorted by their downstream interaction. According to our own observations as well as the results of Spivack (1946), Bearman & Wadcock (1973), Zdravkovic (1977) and Beguier *et al.* (1977) this spacing is sufficient to produce no noticeable coupling of the vortex shedding of the two individual cylinders. After the screens and honeycomb were placed in the settling chamber of the wind tunnel, turbulence intensity in the test section was as low as 0.055%. Freestream velocity in these experiments was $U_R = 6.46$ m s^{-1}. The pressure-drop coefficient along the 2.54 m of the test section where the interacting wake was studied was only $C_p = \Delta P/\frac{1}{2}U^2 = 0.0362$. Pressure gradients of such small magnitude are not expected to influence noticeably the dynamics of the turbulence in the wakes. Freestream temperature fluctuations were virtually non-existent. Noise elimination from the temperature signal reduced the apparent r.m.s. level to only 0.0014 °C. Use of the freestream temperature probe, the signal of which was subtracted from the wake temperature signal on an instantaneous basis, contributed to the low noise level. The same was done with the freestream velocity-probe signal, which greatly improved the accuracy of the streamwise velocity profiles, especially at the wake edges.

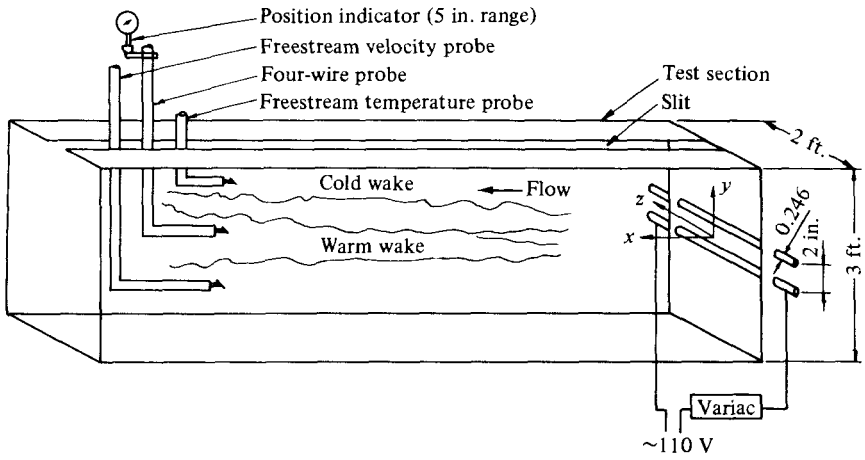

FIGURE 1. Experimental arrangement in the test section.

A special four-wire probe was designed and built by the author. The diameter of all sensors was only 0.625 μm. The probe and the method of processing its signals were described by Fabris (1978). The processing method was based on the simultaneous solution of four nonlinear sensor-response equations. The Newton–Raphson numerical technique was used to solve for mutually uncontaminated instantaneous three velocity components and temperature. Accuracy of the measurements was further improved by accounting for drifts in the d.c. baseline in all channels during data acquisition. 60 Hz conditioned noise was computed and then subtracted from all channels. All analog signals were converted to digital at a sampling rate of 4000 per second. Low-pass filters were set at 2000 Hz to avoid aliasing. Six seconds of real-time signals were processed to calculate flow quantities.

Since the merging 'double' wake is heated asymmetrically, complete profiles were taken. Δy spacing between lateral positions was 7.366 mm at $x/D = 400$ and 6.04 mm at $x/D = 200$. In all, 27 lateral positions were recorded at each downstream location.

The temperature-measuring circuits were developed and tested over an extended period. The result was a very low noise level in the temperature signal. This permitted the use of smaller conditional-sampling discrimination thresholds (only 0.013 °C in our case) than have previously been possible. As discussed by Fabris (1981), systematic changes of the threshold level and the hold time did not produce appreciable change in the computed intermittency factor or the bursting frequency, as was reported by La Rue (1974). Short tongues of colder fluid within heated fluid, discussed by Dean & Bradshaw (1976), were still comfortably above the low threshold level used in this study.

3. Development of the flow

In order to be able to select an appropriate significant downstream location for a detailed conditional-sampling study of the interaction of two wakes, the development of flow was documented using a single-wire probe. In this fashion we obtained the mean streamwise velocity and the root mean square of its fluctuations, which are shown in figures 2 and 3. At the first location, $x/D = 25$, the single wakes are fully separated and distinct. Since we also measured the single wake at that location, we can say that any differences are below the resolving power of the instruments. At $x/D = 50$, the defect at the centre of the double wake is about 8.5% of the local

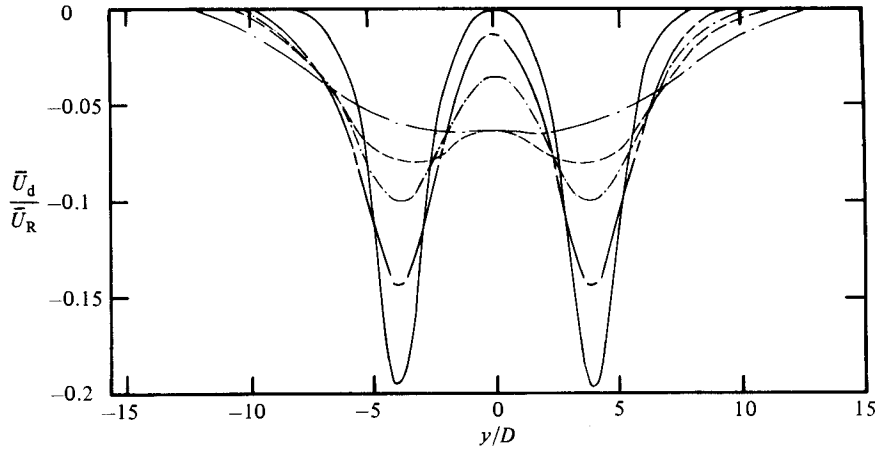

FIGURE 2. Double-wake velocity defect: ——, $x/D = 25$; – –, 50; –·–, 100; – – –, 200; —·—, 400.

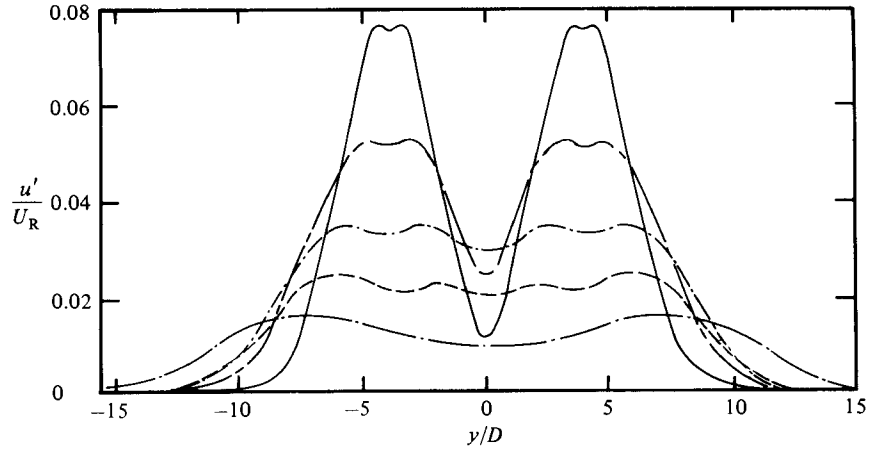

FIGURE 3. u' profiles of double wake: ——, $x/D = 25$; – –, 50; –·–, 100; – – –, 200; —·—, 400.

maximum defect. At $x/D = 100$ it increases to 35 %, but the region of interaction of the individual wakes remains relatively narrow. At $x/D = 200$ the defect at the wake centre grows to 80 % of the local maximum, and the region of wake interaction widens considerably. At $x/D = 400$ the mean defect profiles begin to resemble the defect of a single wake. There is a rather wide region with small shear $\partial\bar{U}/\partial y$; this region and its parameters are significant in the analysis of the turbulence. Away from this central region, the slope $\partial\bar{U}/\partial y$ is comparable to that of the individual single wakes at $x/D = 400$.

An interesting effect, not pursued in detail, is observed in both figures 2 and 3: the outer spreading rate between x/D stations of 100 and 200 is minimal. This is, of course, the region of vigorous early interaction between the opposite shears and of interpenetration of the individual wake bulges, which deserves a separate careful investigation. When the double-wake profile starts to resemble that of the single wake, the outer spreading is resumed.

Figure 3 displays the development of the r.m.s. streamwise velocity fluctuations for the double wake. At $x/D = 25$ the two u' profiles are those of the individual wakes,

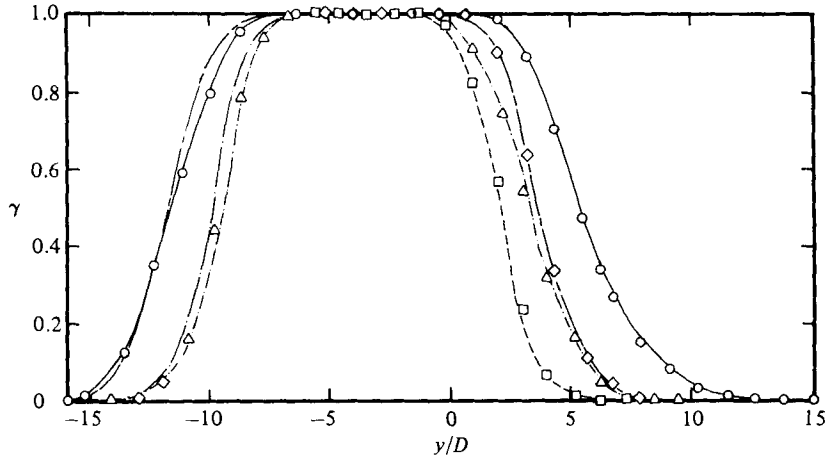

FIGURE 4. Intermittency factor: ○—○, $x/D = 400$, 2 cylinders; ◇---◇, 400, 1 cylinder; △-·-△, 200, 2 cylinders; □--□, 200, 1 cylinder.

each with two separate maxima. Between the cylinders the fluctuations do not drop to the low freestream values. There are, instead, larger-scale potential fluctuations induced by the wakes from both sides. The four u' maxima then decrease steadily with x, while the distance between them increases.

The curious u' profile at $x/D = 200$, and its contrast with that at $x/D = 400$, exhibit the features which led to the choice of the distance between the two cylinders. At $x/D = 200$, the interaction between the maxima and the wake trough is of special interest for these detailed investigations. At $x/D = 400$, the absence of the inner maxima, albeit with a broad region of relatively high u' fluctuations at the centre of the complex double wake, begins to bear a similarity to that of a single wake. Clearly, the as-yet incomplete interpenetration of the two individual wakes at $x/D = 400$, which is best demonstrated by spreading of fluid of increased temperature originating from the lower cylinder, presents an especially intriguing target for the detailed measurements we report here.

The intermittency function was defined as being 1 in heated and 0 in unheated fluid. This definition yields conditional results at the lower side of the complex wake consistent with those in the single wake of Fabris (1979). By such choice of values for the intermittency function it will be possible to infer effects of the second turbulent wake simply by the direct comparison of results at the upper and lower sides of the thermal part of the complex wake. In selected cases, results in the basic, single wake will be provided for contrast.

4. Distributions of intermittent heated and untreated fluid

One of the important pieces of information provided by conditional sampling is the statistical data of intermittent turbulent and potential flow. Since in this study the lower cylinder only was heated, the thermal front was coextensive with the instantaneous boundary of turbulent flow at the lower side of the complex wake. At the upper side of the wake, however, the thermal front was wholly contained within a fully turbulent fluid, which provided the opportunity to investigate some quite subtle characteristics of the interaction between two turbulent flows.

Figure 4 compares directly intermittency factors of the single and the double

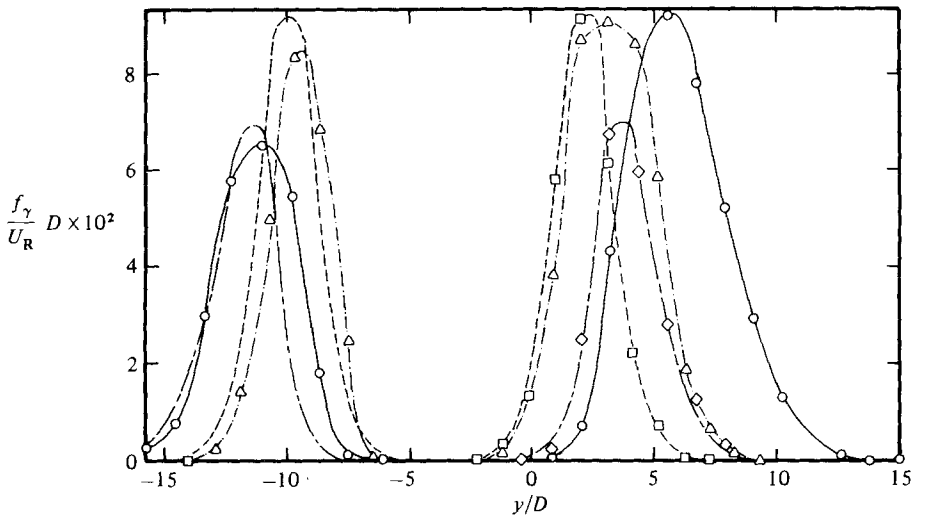

FIGURE 5. Bursting rate: ○—○, $x/D = 400$, 2 cylinders; ◇---◇, 400, 1 cylinder; △-·-△, 200, 2 cylinders; □--□, 200, 1 cylinder.

interacting wakes at $x/D = 200$ and 400. The single-wake flow-field was measured at the upper side only. The curves for its lower side are obtained by symmetrical reflection about the centreline position at $x/D = -4$. Figure 4 reveals that at the lower side the results are very similar for the single and the double wake. There the interface between the heated and unheated fluids coincides with the interface between the turbulent and potential flows. At the upper side the two original single turbulent wakes are interacting, and the thermal interface is wholly within the fully turbulent flow. Figure 4 indicates that interaction of two turbulent flows enhances the mixing process, causing a more pronounced, upward transfer of heat. This upward shift is especially significant for low intermittency factors, suggesting strong lateral penetration of the crests or top positions of the heated turbulent bulges. A plot in probability coordinates is not provided here; however, figure 4 suggests that an approximately Gaussian distribution of γ is retained.

At the lower side, spreading of the double wake is slightly lower than that of the single wake. As noted earlier, this may be a consequence of the interaction of the single wakes. At $x/D = 200$ the extent of the lower sides of the single and double wakes is about equal for all values of γ. At $x/D = 400$ a difference in such spreading exists only for high γ. This could be due to the fact that the double wake seems to resume widening at an even higher rate than the single wake near this downstream position.

Figure 5 compares bursting rates for the single and double wakes. Bursting rate is defined here as the rate at which the fronts of heated bulges cross at a particular position in space. At $x/D = 200$, for example, the maximum bursting rate at the upper side of the double wake has almost the same value as for the single wake, but the curve is wider and has moved upwards. The maximum value at the lower side of the double wake is about 10% lower than for the single wake. On the other hand, at $x/D = 400$ the ratio between maxima of the double and single wakes at the lower side seems to remain about the same as found at $x/D = 200$; while, at the upper side, the peak number of heated bulges in the merging wake is about 20% higher than for the wake. Only 2–4% of this increase can be attributed to higher convection velocity. The data suggest, instead, that the turbulent-to-turbulent fluid entrainment is

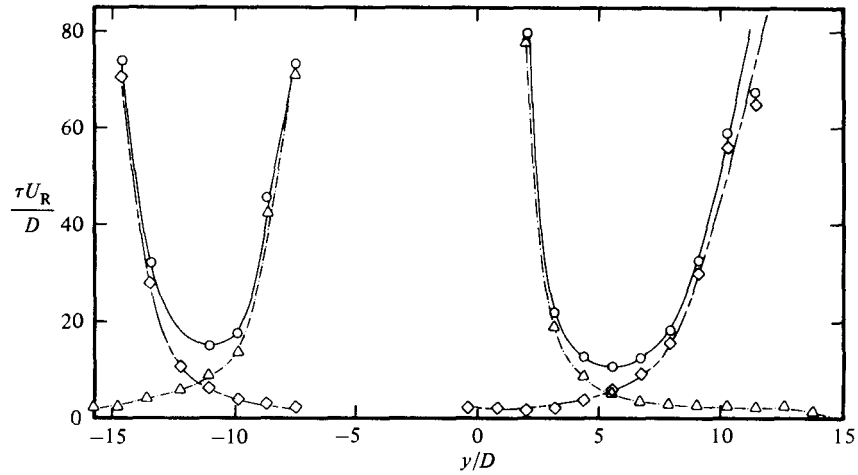

FIGURE 6. Time lengths of intermittency intervals; $x/D = 400$, 2 cylinders: ○—○, back–back; ◇– –◇, back–front; △–·–△, front–back.

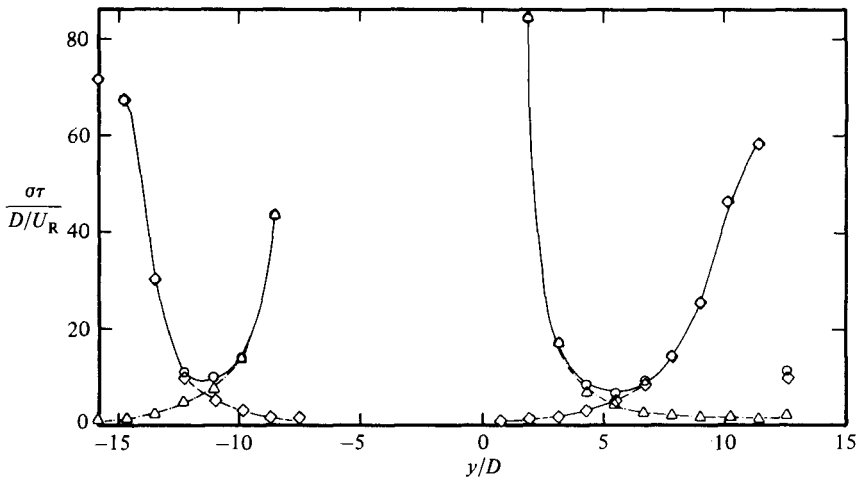

FIGURE 7. Standard deviation of intermittency intervals; $x/D = 400$, 2 cylinders: ○—○, back–back; ◇– –◇, back–front; △–·–△, front–back.

preferential in this case or occurs in such a way that not only do lateral undulations of the thermal interface increase, but also the interface becomes more corrugated.

Statistical properties of heated- and cold-fluid intermittent time intervals were also computed. 'Complete-cycle' intervals were also studied by noting the elapsed time between passage of the backs of two consecutive heated bulges. Thomas (1973) also studied front–front time intervals and found that their statistical behaviour did not differ appreciably from back–back intervals. Figure 6 displays the average durations of the intermittent time intervals. General trends are as expected, with the 'full' intervals being the shortest at the $\gamma = 0.5$ location. In the interacting region the local minimum of duration of the full intervals is 10.5, while at the lower side it is 15. The previous two figures suggest that the integral scale of turbulence decreases in the interaction process; which is contrary to the expectation, however, that the scale of turbulence grows as a function of the width transformations in the mean velocity profile. Standard deviations of the time intervals are given on figure 7. They exhibit trends similar to those of the average durations.

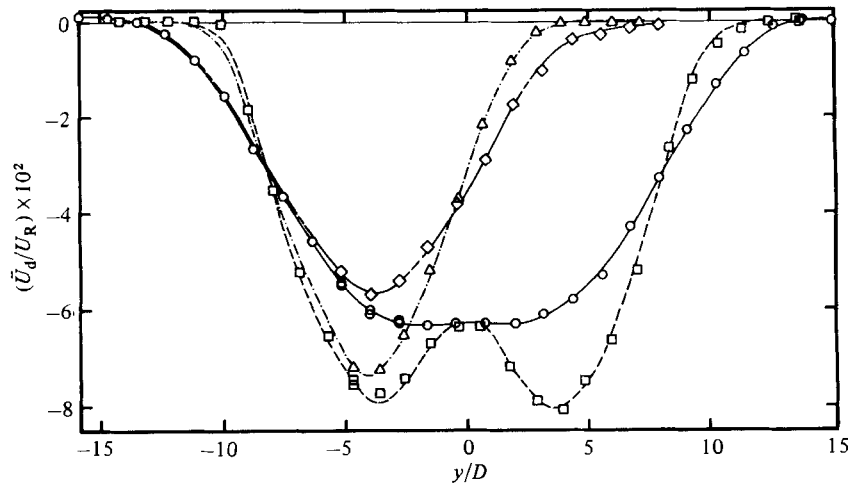

FIGURE 8. Conventional mean streamwise velocities: ○—○, $x/D = 400$, 2 cylinders; ◇−·−◇, 400, 1 cylinder; △−·−△, 200, 1 cylinder; □−−□, 200, 2 cylinders.

5. Mean-flow quantities

5.1. *Streamwise velocity*

Figure 8 compares the streamwise velocity profiles of the single and double wakes at two downstream locations. As noted above, the double wakes were so broad that the traversing had to be accomplished in two segments, with overlaps of three datum points. For the single wake, the lower parts of the profiles, without indicated points, are simply reflections with respect to the centreline sketched in to aid the reader in making comparisons.

The single-cylinder wake defect decreases from its maximum of 7.4 % at $x/D = 200$ to 5.7 % at $x/D = 400$, while the wake in the same interval widens. The double wake defect at $x/D = 200$ exhibits two distinct maxima corresponding to the original individual wakes. The double wake at $x/D = 400$ is of course wider than at $x/D = 200$, and has an almost flat profile at the centre. These double-wake profiles show that the x/D positions were chosen appropriately, since at $x/D = 200$ the interaction between the two wakes is already significant and at $x/D = 400$ the interaction is at its maximum, Further downstream the double-wake structure relaxes toward single-wake behaviour.

Bragg & Seshagiri (1973) and Beguier, Giralt & Keffer (1978) postulated that the velocity profiles in the interaction of a far turbulent wake can be approximated by the linear superposition of velocity-defect profiles of the individual wakes. When this superposition is performed at $x/D = 400$ the combined velocity profile is found to have a higher spiked maximum at the centreline. From this it can be inferred that the linear-superposition hypothesis is a good approximation only in the early, weak stages of the interaction process.

In the flat region at $x/D = 400$ the dominant term $\overline{uv}\,\partial\bar{U}/\partial y$ in the production of turbulence becomes insignificant, and it is the rate of decay of turbulence and diffusion in that region which then becomes of special interest.

The measured maxima of the two lobes at $x/D = 200$ differ by 5 %. Our analog measurements in the cold wakes gives this difference to be three percent. The additional discrepancy of 2 % is probably associated with the finite averaging times

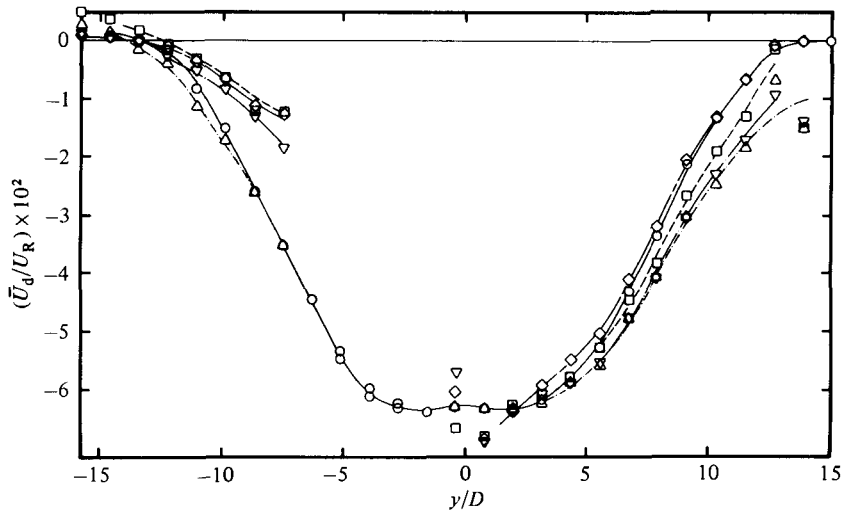

FIGURE 9. Conditional streamwise velocities; $x/D = 400$, 2 cylinders: ○—○, conventional; ◇–·–◇, unheated zones; △–·–△, heated zones; □–·–□, heated fronts; ▽–·–▽, heated backs.

during the traverses. This approximation was accepted in order that data acquisition and processing not become economically prohibitive. The above discrepancies are given in terms of very small velocity defects rather than in terms of the actual streamwise velocities, which are nearly twenty times larger.

Figure 9 shows the streamwise conditional velocity defects. As explained earlier, on the lower side of the wake the heated flow interface coincides with the turbulent–potential-flow interface, giving almost the same results as for the single warm wake, which could be used as a reference. On the upper side, however, the temperature interface is wholly within the fully turbulent region. On the upper side, the unheated flow average at any particular position can thus comprise both turbulent and potential-flow contributions.

On the upper side, the cold flow is moving faster than the conventionally averaged flow, while the heated flow is moving slower, and in this case, interestingly, the difference is more pronounced than in the single-cylinder case. One might find this surprising, since the unheated flow includes the slower, turbulent flow. The explanation of this phenomenon derives from the fact that the heated flow coincides with 'old' turbulence coming from the centre of the double wake, i.e. with fluid lumps of lowest streamwise momentum. Just as in the single wake, the fronts of the heated bulges are moving faster than the backs, indicating a net streamwise spreading of the heated regions at all locations. However, in this case, the fronts are not moving faster than the cold-fluid zones.

5.2. *Lateral velocity*

Figure 10 shows the conditional lateral velocities. The heated- and unheated-flow zone averages behave as in the single-wake case in Fabris (1979). In the lower half of the double wake the front and back point averages also follow the pattern of the single-wake case, but do show a distinct difference in the region of interaction with the upper cold wake. At the upper wake boundary both point averages are positive, while at the centreplane both are negative; they cross in the outer reaches of the upper cold wake. In contrast with the behaviour of the single wake in Fabris (1979), these

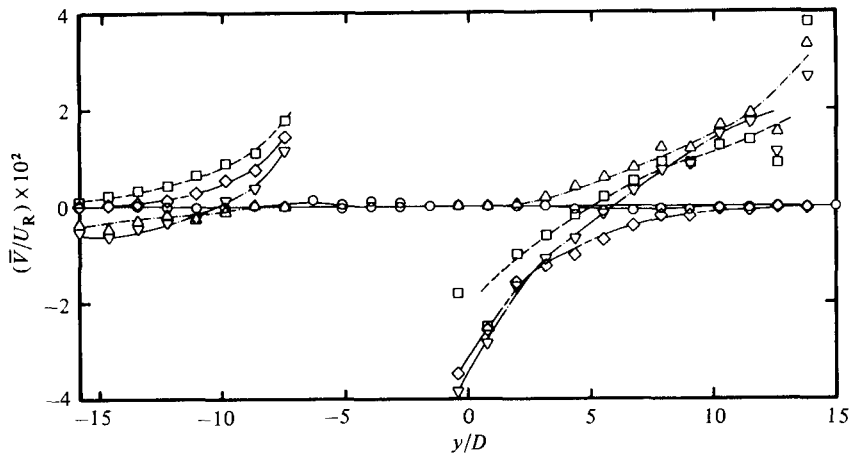

FIGURE 10. Conditional lateral velocity; $x/D = 400$, 2 cylinders: ○—○, conventional; ◇--◇, unheated zones; △-·-△, heated zones; □--□, heated fronts; ▽-·-▽, heated backs.

point averages are more positive than the unheated-zone averages (except near the centreplane). On the other hand, the behaviour of all the averages on the lower side of the double wake in figure 10 is consistent with that of the corresponding averages for the single wake ('antisymmetric reflections' plus change in scale).

Figure 11 provides a direct comparison of lateral velocities in heated and cold zones for the single and double wake. The magnitudes are 2–3 times larger for the double-wake case in the upper interaction region. This is directly opposite to the commonly accepted belief advanced by Bragg & Seshagiri (1973) that turbulent bulges from the two separate wake 'collide' and bring the lateral velocity to zero. It shows that large-scale motion in the interaction region actually enhances mixing. J. Foss and S. Corrsin (1974, private communication) have observed that a heated interface in a uniform turbulent flow spreads faster than if the unheated coflowing region were only potential. Here the larger-scale motion seems to add still another factor. It is as is the turbulent bulges or contrarotating eddies of the two wakes reinforce each other.

5.3. *Temperature*

Figure 12 compares the conventionally averaged temperatures of the single and double wakes at two downstream locations. The single-wake temperature profile has broader peaks than those of the double wake. This is in contrast with the behaviour of the velocity defects in figure 8. However, at the edges of the single wake the velocity defect spreads wider than does the mean-temperature profile.

In the case of the double wake the temperature spread is significantly greater in the upper interaction region, especially at $x/D = 400$. However, the excess heat so spread is not large. One should bear in mind that the spreading rates relative to mean streamlines could be larger, in the case of the double wake, throughout the entire region.

Figure 13 displays the conventionally and conditionally averaged temperatures in the double wake. Clearly, the interaction with the upper, cold wake spreads the heat outward much further, but the averages of the heated lumps are significantly decreased with respect to those at the edge of the lower, heated wake here as well

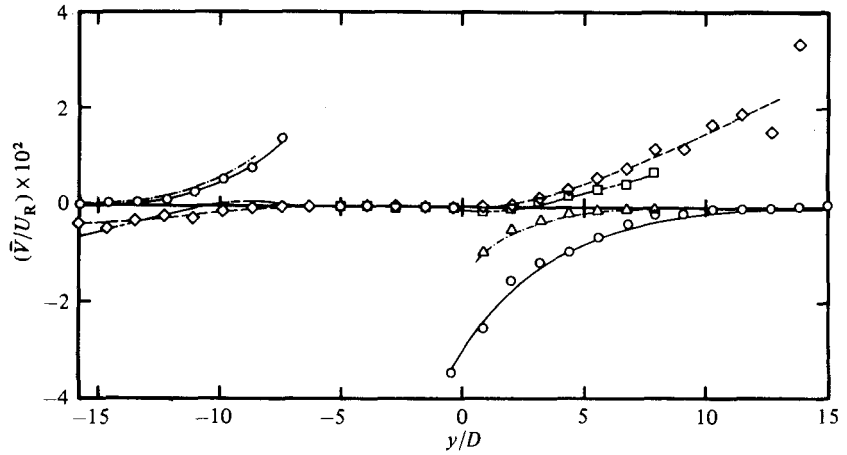

FIGURE 11. Conditional lateral velocities; $x/D = 400$; ○—○, unheated zones, 2 cylinders; ◇–·–◇, heated zones, 2 cylinders △–·–△, unheated zones, 1 cylinder; □–□, heated zones, 1 cylinder.

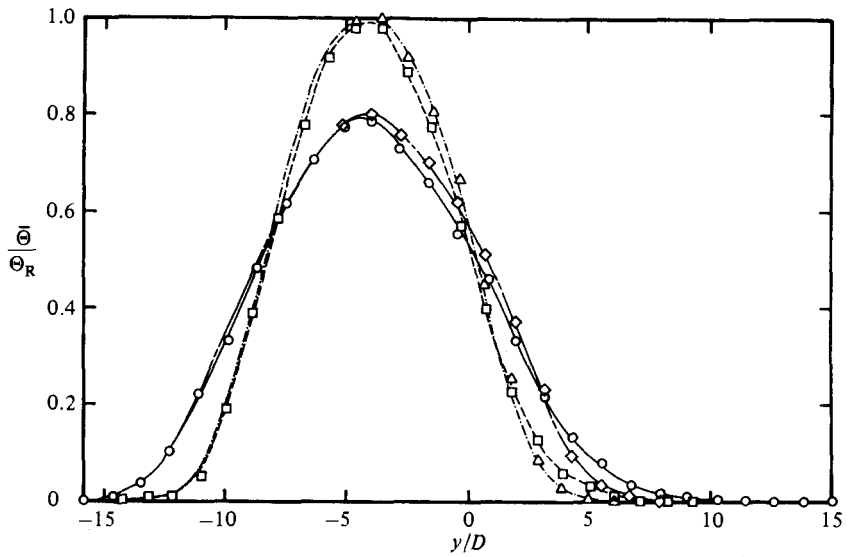

FIGURE 12. Mean temperature: ○—○, $x/D = 400$, 2 cylinders; ◇–·–◇, 400, 1 cylinder; △–·–△, 200, 1 cylinder; □–□, 200, 2 cylinders.

as in figure 12. No appreciable difference between the point averages of backs and fronts can be noticed in the upper mixing region. Also these point averages hardly change with lateral position.

For easier comparison, figure 14 presents the conventional and heated-zone averages for the single and double wakes on one graph. Many of the features discussed above can be seen more clearly in this mode of presentation.

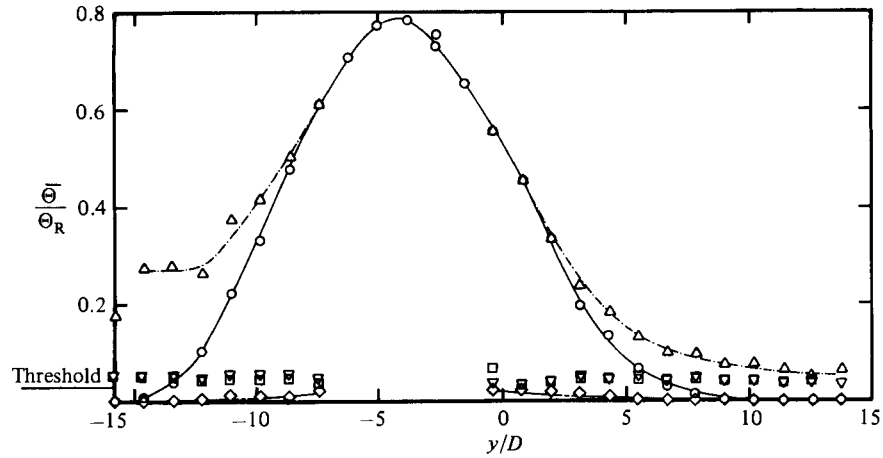

FIGURE 13. Conditional mean temperatures; $x/D = 400$, 2 cylinders: ○—○, conventional; ◇---◇, unheated zones; △-·-△, heated zones; □, heated fronts; ▽, heated backs.

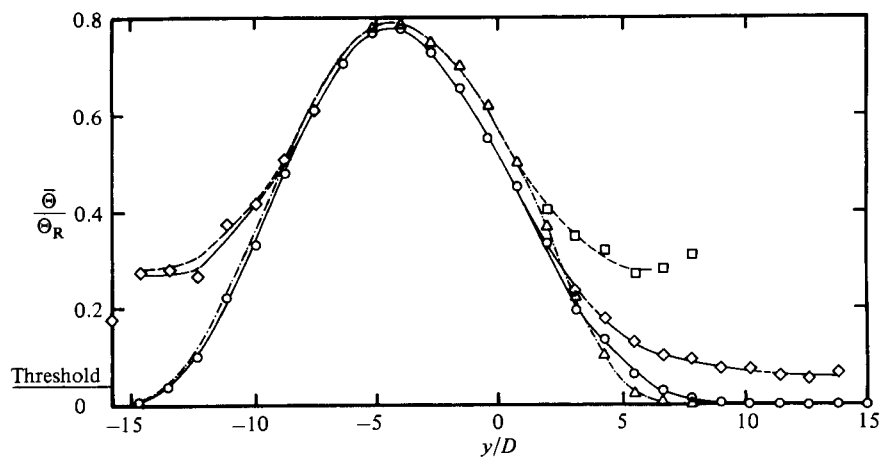

FIGURE 14. Conditional mean temperature; $x/D = 400$: ○—○, conventional, 2 cylinders; ◇-·-◇, conventional, 1 cylinder; △-·-△, heated zones, 2 cylinders, □--□, heated zones, 1 cylinder.

6. Fluctuating quantities – mean squares

In this section we will present the profiles of mean squares of the fluctuating quantities $\overline{u^2}$, $\overline{v^2}$, $\overline{w^2}$, $\overline{\theta^2}$ and $\overline{q^2}$. As discussed earlier, there are at least three ways of computing such fluctuations. Only those that have a physical interpretation will be described here.

6.1. *The streamwise fluctuations*

The conditional squared streamwise velocity fluctuations computed with respect to conventional mean velocity (R-averaging) are given in figure 15. The conventional curve shows peaks which are somewhat lower than those for the single wake. They occur further apart, but again correspond to the region of maximum mean strain rate (cf. figure 9). It is most significant that the conventional $\overline{u^2}$ distribution is symmetrical,

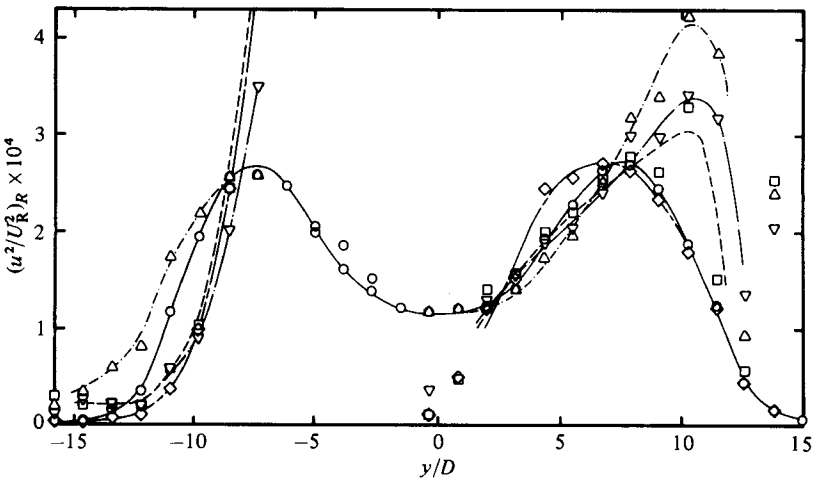

FIGURE 15. Conditional streamwise fluctuations; $x/D = 400$, 2 cylinders, R-average: ○—○, conventional; ◇---◇, unheated zones; △-·-△, heated zones; □--□, heated fronts; ▽-·-▽, heated backs.

within the precision of the measurements. Thus the differential heating has a negligible effect on the dynamic turbulence field. Also the sensitivity of the hot wires to temperature is apparently negligible, again within the precision of the measurements. The level of turbulence at the centreplane is substantially lower than the maximum, suggesting a lack of production, decay or depletion of $\overline{u^2}$ energy through diffusion.

The cold-zone average reaches its maximum at almost the same level as the conventional average. However, it exceeds the conventional average just where the cold-zone defect $\overline{U}_d$ shifts inward with respect to the conventional $\overline{U}_d$ average in figure 9. Figure 9 discloses why the heated-zone defect curve is displaced outward – the warm lumps have been slowed in their penetration of the cold upper wake. It is curious that the fluctuations in the heated lumps follow this outward shift of their mean defect. This conditional average is significantly higher and is shifted outward. The unheated-zone averages on the lower side of the double wake display no such behaviour, because the cold lumps migrating from the upper cold wake do not remain cold, i.e. below the threshold. Thus, despite the presence of these slow formerly cold lumps, the statistics of the lower part of the double wake follow essentially the behaviour of those in the single wake. The trends for $y/D < -8$ in figure 15 resemble the trends in the single wake for $y/D > 5$ (in Fabris 1979). The curve for the fronts and backs of the heated regions are not shown, but they basically follow the variations in the heated and unheated zones.

Figure 16 gives the same fluctuations, but computed with respect to appropriate zone conditional means. The results remain similar to the standard averages in figure 15. Although the Z-averages are, by definition, smaller, the peak in the heated fluid is still the highest and it is still shifted outward. Both presentations convey useful information. At the lower side of the double wake, the turbulent fluid seems to be somewhat less energetic, but otherwise the trends are similar to those in the case of the single cylinder.

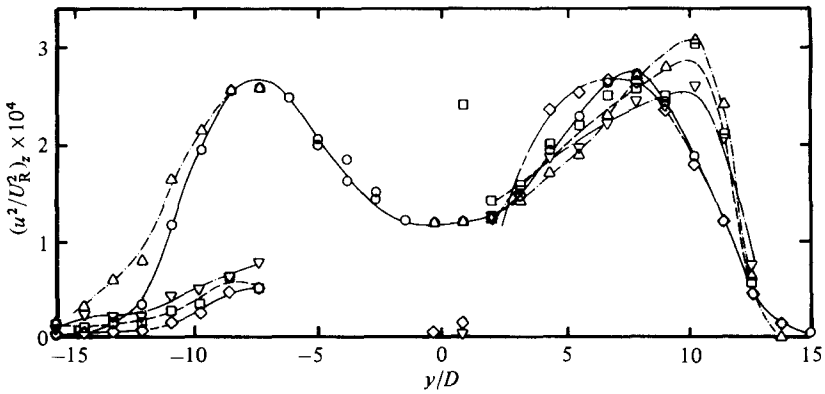

FIGURE 16. Conditional streamwise fluctuations; $x/D = 400$, 2 cylinders, Z-average: ○—○, conventional; ◇–·–◇, unheated zones; △–··–△, heated zones; □–·–□, heated fronts; ▽–··–▽, heated backs.

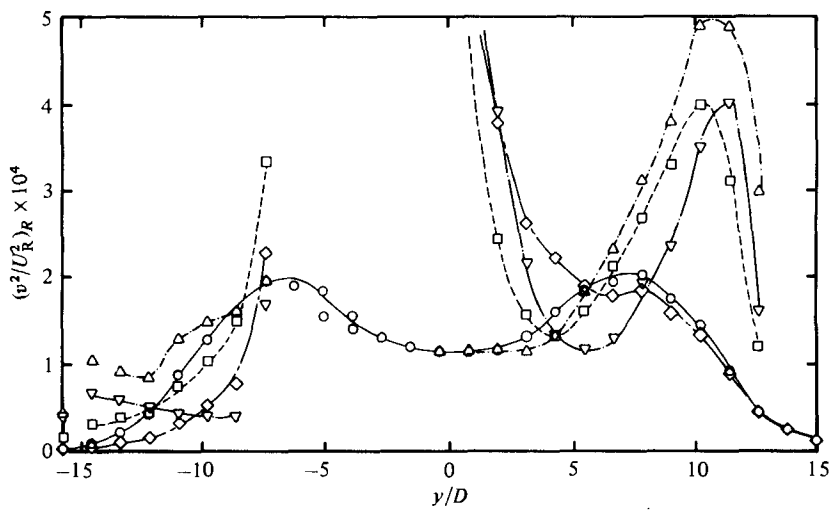

FIGURE 17. Conditional lateral fluctuations; $x/D = 400$, 2 cylinders: ○—○, conventional; ◇–·–◇, unheated zones; △–··–△, heated zones; □–·–□, heated fronts; ▽–·–▽, heated backs.

6.2. *The lateral fluctuations*

Figure 17 displays the variation of the lateral fluctuations. The most interesting features are the high R-averages in the cold potential fluid penetrating close to the centreline and in the warm fluid at the upper edge of the wake. The cold $\overline{v^2}$ averages thus differ from the $\overline{u^2}$ averages in figure 15 near the centreplane. The outward shift of the maxima of the fluctuations in the warm lumps follows the shift of the corresponding averages of $\overline{U}_d$ and $\overline{u^2}$ in figures 9 and 15 respectively.

The fluctuations of the fronts and backs of the heated zones again basically follow those of the local 'minority zones', i.e. the cold averages near the centreplane and the hot averages at the upper edge of the wake. At the lower edge of the double wake, the trends in all the averages are similar to those for the single wake. No separate diagram is provided for Z-averages, but some of them are indicated by full symbols on figure 17. Z-averaging yields significantly decreased peaks. On the upper side,

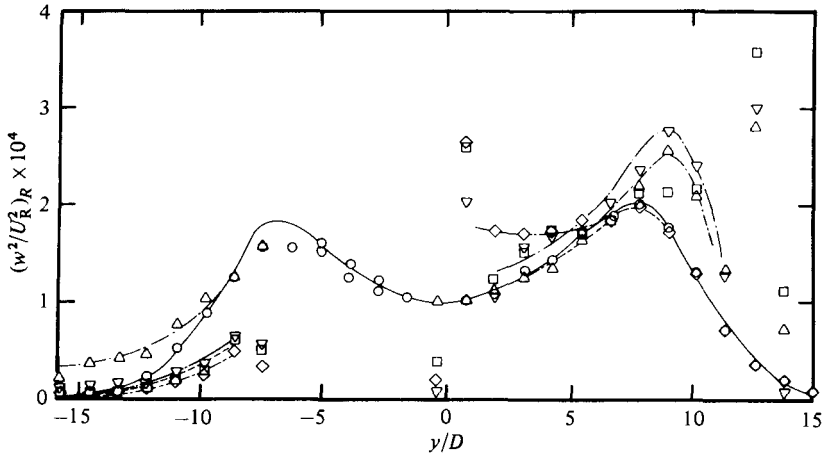

FIGURE 18. Conditional spanwise fluctuations; $x/D = 400$, 2 cylinders, R-average: ○—○, conventional; ◇−−◇, unheated zones; △−·−△, heated zones; □−−□, heated fronts; ▽−·−▽, heated backs.

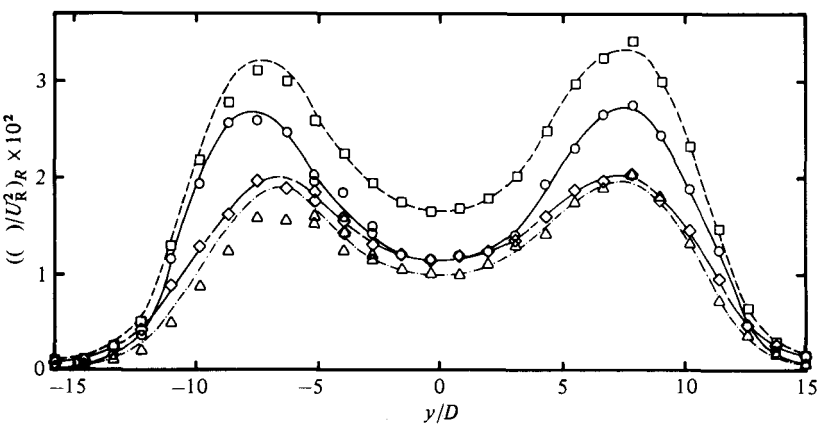

FIGURE 19. Turbulent energy; $x/D = 400$, 2 cylinders, R-average: ○—○, $\overline{u^2}$; ◇−−◇, $\overline{v^2}$; △−·−△, $\overline{w^2}$; □−−□, $\frac{1}{2}\overline{q^2}$.

however, the heated zones still have the highest relative maximum which is shifted outward.

It is interesting to note that, despite the asymmetric heating of the double wake, the conventional $\overline{v^2}$ averages are symmetric within the precision of the data.

6.3. *The spanwise fluctuations*

Figure 18 shows that the unheated fluid maintains an almost constant level in the inner part of the wake. The heated bulges again exhibit a higher level of fluctuation at the wake's periphery. However, the warm peaks are displaced outward less than the $\overline{u^2}$ and $\overline{v^2}$ cases, a behaviour which is consistent with the aforementioned degree of two-dimensionality. There is a substantial trough in the turbulent energy contribution in the centre of the double wake, as was discussed in the analysis of figure 15.

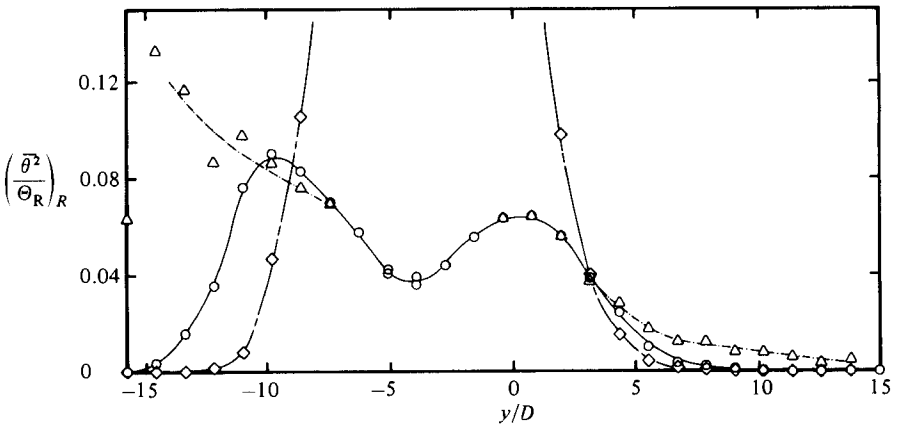

FIGURE 20. Conditional temperature fluctuations; $x/D = 400$, 2 cylinders; ○—○, conventional; ◇–·–◇, unheated zones; △–·–△, heated zones.

6.4. *Kinetic energy of fluctuations*

Figure 19 compares the three components of the conventionally averaged fluctuations, as well as the turbulent kinetic energy

$$\tfrac{1}{2}\overline{q^2} = \tfrac{1}{2}(\overline{u^2} + \overline{v^2} + \overline{w^2}).$$

All the components of energy show peaks at the location of strongest shear $\partial\overline{U}/\partial y$, with $\overline{u^2}$ possessing the highest value, since it is first to receive newly produced turbulent energy. Of the three components, $\overline{v^2}$ is seen to undergo the least proportional variation across the double wake, being relatively higher than the other components at the centreline and edges. This is consistent with Phillips' (1955) theory of a slower decay in potential $\overline{v^2}$ fluctuations outside a stationary two-dimensional turbulent flow. A wide energy-deficient trough in the middle where the two individual wakes interact is a dominant feature which should make a useful target for predictive models and theories of shear turbulence.

6.5. *Temperature fluctuations*

Figure 20 gives conditional temperature fluctuations. Obviously the temperature fluctuations in the heated bulges in the upper part of the wake are now at a much lower level than in the single wake. In the lower part of the wake the levels and general features show very little difference from those of the single wake. There is, however, considerably more mixing and entrainment in the double wake than in the single wake. The ultimate explanation of the lower $\overline{\theta^2}$ level in the upper part of the double wake must take into account the full energy budget, according to Tennekes & Lumley (1972, p. 95).

Z-averages are indicated by full symbols. The change as compared with R-averages is minor for the heated bulges at the upper side of the wake.

Figure 21 provides a direct comparison of the distributions in the single and double wakes. Here the lack of effect at the lower wake (i.e. at the level of the heated cylinder) is remarkable. The near-mirroring of the Z-averaged fluctuations in the warm parts of the single wake, near $y/D = 2$, and of the lower part of the double wake, near $y/D = -10$, should also be significant for the first-order effects. The closeness of the conventional average to the warm Z-average in the upper part of the double wake

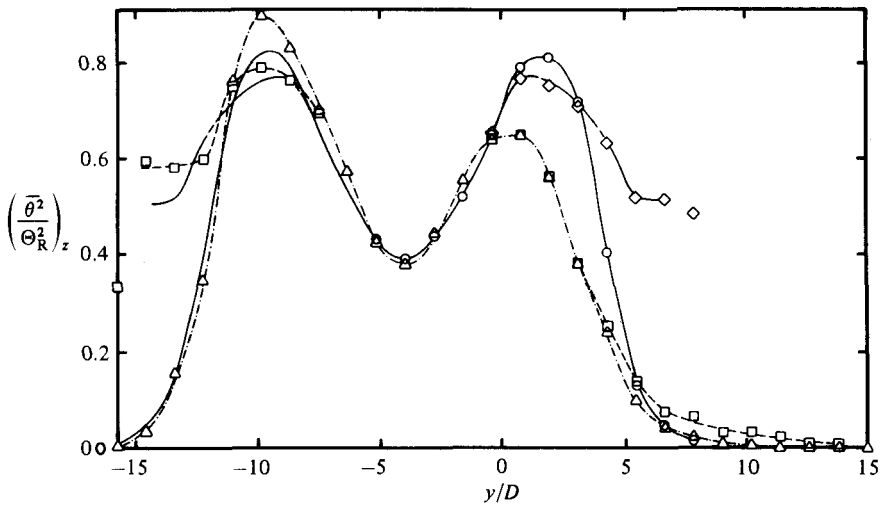

FIGURE 21. Temperature fluctuations; $x/D = 400$, Z-average: ○—○, conventional, 1 cylinder; ◇---◇, heated zones, 1 cylinder; △-·-△, conventional, 2 cylinders; □--□, heated zones, 2 cylinders.

contrasts with their divergent behaviour in the lower part of the wake. Again, this contrast should hold important clues for the predictors: it may well distinguish between proposed assumptions.

7. Summary and conclusions

A complex turbulent flow was formed by the merging of two simple two-dimensional far-turbulent wakes. The slight heating of only one of the basic single wakes traced its fluid by an elevated temperature and permitted the use of the conditional-sampling technique to investigate the merging process. A special four-wire probe made by the author and a method of processing of its signals described by Fabris (1978) enabled the simultaneous and precise measurements of uncontaminated instantaneous u, v, w and θ. The preliminary diagnostic experiments described by Fabris (1979) contributed substantially to the accuracy of the data reported here.

The merging interacting wake is a developing flow which has not been previously documented in detail. As such, it is an intriguing subject for fundamental studies concerning the nature of turbulence, and for providing data to test and further develop prediction methods.

Some interesting findings are as follows:

1. Mean velocities and fluctuating fields developing rapidly in the interacting region at $x/D = 200$ and 400 are coupled with diminishing turbulent energy.

2. The lateral spreading of the heat of the single heated wake is enhanced due to its interaction with another equal but unheated wake.

3. Corrugation of the thermal interface is significantly increased in terms of wider lateral undulations and shortened streamwise periods than in the basic single wake.

4. The heated fluid exhibits somewhat more pronounced slower differential streamwise movement compared with the conventional fluid than is the case in the single basic wake.

5. The mutual lateral countermovement of heated and unheated bulges is two to

three times faster in the complex wake than is the vase for the basic wake in which the unheated fluid is potential. It appears that the counter-rotating large eddies of two merging single wakes amplify each other's lateral movements.

6. Significantly lower mean and fluctuating temperature levels were observed in the intermittent turbulent fluid on a conditional basis. This is a reflection of a higher entrainment rate in turbulent/turbulent interactions.

7. Significantly higher conditional than conventional maxima of all three components of turbulent kinetic energy were observed. These maxima are located further outwards and appear to be associated with an outward shift of conditional $\partial\overline{U}/\partial y$ for heated zones.

The author is indebted to Professors M. V. Morkovin, A. A. Fejer and J. L. Way for their guidance and support. Critical reviews by the referees are very much appreciated.

REFERENCES

Andreopoulos, J. & Bradshaw, P. 1980 *J. Fluid Mech.* **100**, 639.

Bearman, P. W. & Wadcock, A. J. 1973 *J. Fluid Mech.* **61**, 495.

Beguier, C., Giralt, F., Fulacher, L. & Keffer, J. F. 1977 In *Proc. Symp. on Turbulence, Berlin.*

Beguier, C., Giralt, F. & Keffer, J. F. 1978 In *Proc. 6th Intl Heat Transfer Conf., Toronto,* p. 353.

Bradshaw, P. 1976 In *Proc. 1976 Heat Transfer and Fluid Mech. Inst., Davis, California.*

Bragg, G. M. & Seshagiri, B. V. 1973 *Intl J. Heat Mass Transfer* **16**, 1531.

Chevray, R. & Kovasznay, L. S. G. 1969 *AIAA J.* **7**, 164.

Dean, R. B. & Bradshaw, P. 1976 *J. Fluid Mech.* **78**, 641.

Domptail, C., Bonmarin, P. & Dumas, R. 1978 In *Proc. 15ème Coll. d'Aerodyn. Appl., Marseille, France.*

Fabris, G. 1978 *Rev. Sci. Instrum.* **49**, 654.

Fabris, G. 1979 *J. Fluid Mech.* **94**, 673.

Fabris, G. 1981 In *Proc. 3rd Turbulent Shear Flow Symp., Davis, California.*

Fabris, G. & Fejer, A. A. 1974 *Trans. ASME* I: *J. Fluids Engng* **96**, 92.

Hanjalic, K. & Launder, B. E. 1972 *J. Fluid Mech.* **51**, 301.

La Rue, J. C. 1974 Ph.D. dissertation, University of California at San Diego.

Libby, P. A. 1976 *Phys. Fluids* **17**, 1956.

Palmer, M. D. & Keffer, J. F. 1972 *J. Fluid Mech.* **53**, 593.

Phillips, O. 1955 *Proc. Camb. Phil. Soc.* **51**, 220.

Pope, S. B. 1983 In *Proc. AIAA 21st Aerospace Sci. Meeting, Reno, Nevada.*

Spivack, H. M. 1946 *J. Aero. Sci.* **13**, 289.

Tennekes, H. & Lumley, J. L. 1972 *A First Course in Turbulence.* MIT Press.

Thomas, R. M. 1973 *J. Fluid Mech.* **57**, 549.

Weir, A. D., Wood, D. H. & Bradshaw, P. 1981 *J. Fluid Mech.* **107**, 237.

Zdravkovic, M. M. 1977 *Trans ASME* I: *J. Fluids Engng* **99**, 618.